Materials Advances

ROYAL SOCIETY OF CHEMISTRY

PAPER

View Article Online
View Journal | View Issue

Cite this: *Mater. Adv.*, 2024, 5, 7413

The deployment of an NOTT-300 (Al) MOF thin film as a NO_2 capacitive sensor under ambient conditions†

Mohamed Rachid Tchalala,[a] Osama Shekhah,[a] Youssef Belmabkhout,[a] Hao Jiang,[a] Khaled N. Salama *[b] and Mohamed Eddaoudi *[a]

Received 10th July 2024,
Accepted 9th August 2024

DOI: 10.1039/d4ma00701h

rsc.li/materials-advances

Herein we report on the fabrication of a metal–organic framework (MOF)-based sensor using an NOTT-300 (Al) MOF thin film, deposited as a sensing layer on an interdigitated capacitive electrode (IDE), and deploy it for the detection of nitrogen dioxide (NO_2) at room temperature. The fabricated MOF-based sensor was tested and it demonstrated a significant detection sensitivity for NO_2 with concentrations down to 250 ppb, with a lower detection limit around 4.0 ppb. The NOTT-300 (Al) MOF sensor also displayed an outstanding NO_2 sensing stability and a highly desirable detection selectivity towards NO_2 *vs.* other common gases such CO_2 and H_2O as well.

Introduction

Nowadays, the demand for practical gas sensors is emerging and becoming a key research ground in various areas, especially for industrial applications. Therefore, there is continuously a high need for such gas sensors on sites such as in oil/gas field platforms and refineries.[1,2] Additionally, there are an unlimited number of applications of gas sensors in different sectors like environmental monitoring, food quality control, and toxic, flammable, and combustible gas detection, in addition to health sector applications.[3–5]

Nitrogen dioxide (NO_2) is considered as a badly toxic gas that is typically produced as a byproduct of the burning of chemicals like hydrocarbons. Among others, internal combustion engines and thermal power stations are the key sources of NO_2.[6,7] Other sources comprise petroleum and metal refining industries, electricity generation from coal-based power stations, and wastewater treatment plants.[6,7] As a result, NO_2 sensing has assumed great importance due to the serious problem of air pollution caused by auto exhaust and other sources. Inhaling NO_x affects the respiratory system causing airway infection and severe respiratory problems.[8] Accordingly, the American health safety standards accepted a threshold limit value (TLV) of 3 ppm for short exposure to NO_2.[8] Consequently, it is of great importance to develop highly sensitive and selective NO_x sensors that possess also fast response and recovery kinetics for practical monitoring purposes.

In addition to carbon nanotubes, some metal-oxide nanowires have been explored and found to be promising candidates as highly sensitive chemical sensors.[9–13] Oxide semiconductor-based gas sensors have been extensively researched in detecting several combustible, toxic, and odorless gases.[13] The sensing mechanism was mainly based on detecting a fast change in the conductivity of the oxide semiconductors, as a result of the formation and annihilation of oxygen vacancies in the presence of an oxidizing and/or a reducing gas.[10–14] For example, nanostructured WO_3 sensing materials were reported as some of the best NO_2 sensing materials.[14] Commercially used NO_2 sensors for monitoring diesel exhaust gases contain a porous platinum (Pt) sensing electrode accompanied by a dense zirconia-based electrolyte. However, Pt is also an active catalyst for oxygen reduction, which can obstruct the accurate detection of NO_2 at concentrations below 100 ppm.[14,15] These limitations are driving the research on exploring and developing alternative approaches for NO_2 sensing as developments in diesel engine technology are causing lower NO_2 emissions.

The recent advancement of society sets a firmer requisite for gas sensor performances including flexibility, high sensitivity, lower power consumption, low cost, and easiness of integration with other devices. Therefore, interdigitated electrodes (IDEs) have gained more attention in the last couple of decades owing

[a] *Functional Materials Design, Discovery, and Development Research Group (FMD[3]), Advanced Membranes and Porous Materials Center (AMPMC), Division of Physical Sciences and Engineering (PSE), King Abdullah University of Science and Technology (KAUST), Thuwal 23955-6900, Kingdom of Saudi Arabia. E-mail: mohamed.eddaoudi@kaust.edu.sa*

[b] *Sensors Lab, Advanced Membranes & Porous Materials Centre (AMPMC), Division of Computer, Electrical and Mathematical Sciences and Engineering (CEMSE), King Abdullah University of Science and Technology (KAUST), Thuwal, 23955-6900, Kingdom of Saudi Arabia*

† Electronic supplementary information (ESI) available. See DOI: https://doi.org/10.1039/d4ma00701h

to their attractive properties and their unique flexible structural design of different configurations that has improved their chemical or biological sensing properties.[16] The use of lithography in the fabrication process has made the miniaturization procedure simpler and reduced the cost of IDE sensor construction. In turn, this permitted their easy integration with electronics and made the work with the low volume of samples possible. Therefore, the application of IDEs made it possible to satisfy the prerequisite for low-power sensing platforms, such as lab-on-chip applications.[17]

The unique properties of metal–organic frameworks (MOFs), which are considered the new generation of crystalline porous materials, made them potential candidates with significant prospects for addressing current challenges pertinent to energy and environmental sustainability.[18–20] Their unique tunability in terms of design and functionality has made them suitable candidates as effective sensing layers for exploration in various sensing applications.[21–23]

MOFs have recently been used as sensor layers for gas detection systems like H_2S, NH_3, CO_2, SO_2, and other vapours; however, NO_x MOF-based sensors remain an area that has not been highly explored.[24–26] Probably, MOFs have not been widely applied for NO_2 detection because the majority of them did not show unique properties in terms of stability, affinity, and recyclability. Delightfully, the recently discovered aluminum-based Al-NOTT-300 (MOF NOTT-300 (Al) MOF)[27] fulfilled these requirements and therefore we have chosen this MOF, especially due to its reversible adsorption of NO_2 under ambient conditions and high uptake at 1.0 bar and 298 K. Prominently, it shows an exceptional selective removal of low concentration NO_2 (5000 to <1 ppm) from gas mixtures. The NOTT-300 (Al) MOF is a 3D-open framework, isostructural to its indium[28] and gallium[29] analogues, and comprises infinite *cis* $AlO_4(OH)_2$ octahedral chains bridged by a tetradentate ligand (biphenyl-3,3′,5,5′-tetracarboxylic acid (H_4Bptc)) (Scheme 1). In this structural assembly, OH^- groups stick out into the pores along the metal chains in the helical direction, thereby creating a uniform distribution of free OH^- groups on the surface of the pores. These OH^- groups along with four neighboring CH^- groups from benzene rings provide perfect sites for preferable NO_2 binding, which determines its adsorption selectivity toward NO_2.[27]

Additionally, considering the exceptional thermal and chemical stability of this MOF, and its high adsorption selectivity towards NO_2, we opted to expand our research and explore the Al-NOTT-300 MOF for the sensing of NO_2. We, therefore, targeted the fabrication of the NOTT-300 (Al) MOF as a thin film on capacitive IDEs (Fig. S1, ESI†) to function as the sensing layer (Scheme 1).[27–29]

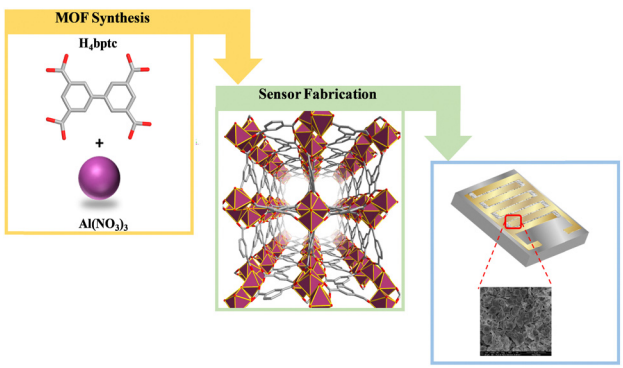

Scheme 1 Schematic representation of the optimized solvothermal preparation approach of the NOTT-300 (Al) MOF and its thin film fabrication on the interdigitated electrodes (IDEs).

Experimental section

Interdigitated electrode fabrication

The IDEs were fabricated using standard complementary metal oxide semiconductor (CMOS) processes. Prior to the growth of the MOF thin film, the substrate underwent cleaning in an ultrasonic bath with acetone, followed by rinsing with isopropyl alcohol (IPA) and DI water. Finally, the fabricated IDEs were cleaned and rinsed extensively with ethanol.[30]

Al-NOTT-300 MOF synthesis

The optimized solvothermal method was used for the synthesis of the NOTT-300 (Al) MOF and was successful, and the obtained material nanoparticles were washed and fully characterized with various techniques. To fabricate the sensing device, an ink was prepared as follows: the NOTT-300 (Al) MOF nanoparticles were suspended in ethanol (4 mg in 1 ml of ethanol) and then spin-coated on the IDE electrode (Scheme 1).

Activating MOF films is crucial to obtain a guest-free film prior to sensing signal measurements. To achieve this, the MOF adsorbent was fully activated by heating it at 85 °C in an oven for 12 hours to remove any residual solvent or water present in the pores.

Materials characterization

Powder X-ray diffraction (PXRD) measurements were carried out using a Bruker D8 ADVANCE X-ray diffractometer with Cu K_α radiation (λ = 1.54178 Å). Field emission scanning electron microscopy (FE-SEM) images were taken on a Quattro Dual Beam microscope at an acceleration voltage of 10 kV.

Sensing experiment

The sensing experiment utilized a custom cell with IDE-loaded with MOF connected to Keysight E4980AL LCR meter. The gas sensing tests were performed using a LabVIEW fully automated measurement system.[29] In our study the MOF coated sensor was placed inside the detection chamber, and using nitrogen gas as a carrier gas the desired concentration of NO_2 was achieved. In this study, we tested the sensor performance in a ppm range from 4 to 100 ppm and a ppb level range from 250 to 1000 ppb.

Testing gas preparation

Gas concentrations were regulated by mixing them with dry nitrogen using a mass flow controller set at a fixed total flow rate of 200 SCCM. For relative humidity measurement, compressed nitrogen was introduced into a water bubbler with temperature control *via* a water chiller, then mixed with dry nitrogen to adjust the relative humidity ratio.

Results and discussion

The coating layer exhibited a homogenous coverage and strong adhesion to the substrate. The crystallinity of the resultant thin film was confirmed by X-ray diffraction (XRD), as shown in Fig. 1a.[29] In addition, the scanning electron microscopy (SEM) images (Fig. 1b and Fig. S1, ESI†) corroborate the formation of a homogenous thin film of these nanocrystals (inset in Fig. 1b).[28] Correspondingly, the successful deposition of the NOTT-300 (Al) MOF crystals directly on the IDE substrate allowed us to deploy it as a capacitive sensor for monitoring and measuring the changes in sensing film permittivity upon exposure to the target gas.[26–28,31–34]

Here we have investigated the sensing properties of the NOTT-300 (Al) MOF thin film on capacitive IDEs for different types of gases/vapours, including NO_2, H_2O, and CO_2. In our study the MOF coated sensor was placed inside the detection chamber, and using nitrogen gas as a carrier gas the desired concentration of NO_2 was achieved. In this study, we tested the sensor performance in a ppm range from 4 to 100 ppm and a ppb level range from 250 to 1000 ppb. Pleasantly, the NOTT-300 (Al) MOF coated sensor was able to perform well in both ppm and ppb ranges, as depicted in Fig. 2(a) and (b). The NOTT-300 (Al) MOF sensors were able to detect NO_2 in the ppb range from 250 to 1000 ppb with a linear response given by the following equation: $Y = 9.32 \times 10^{-4}X + 4.32 \times 10^{-5}$ with a linear fit of $R_2 = 0.987$. However, in the ppm range from 1 to 25 ppm, the curve follows a third-order polynomial behaviour given by the following equation: $4.39 \times 10^{-8}X^3 - 4.0845 \times 10^{-6}X^2 + 1.419 \times 10^{-4}X + 8.066 \times 10^{-4}$, which provided the best match for data description, and the logarithmic fitting gives the coefficient of correlation $R_2 = 1$ (Fig. 2(b)). Most importantly, the NOTT-300 (Al) MOF performed very well at a ppb level down to 250 ppb, with a good linear response (Fig. 2b) and a detection limit of 4.1 ppb. The detection limit at the ppb level was calculated based on the root-mean-square deviation method.[30] Additionally the response and recovery times for NO_2 sensing were calculated from Fig. 2a and found to be fast with values of 178 and 420 seconds, respectively (Fig. S2, ESI†).

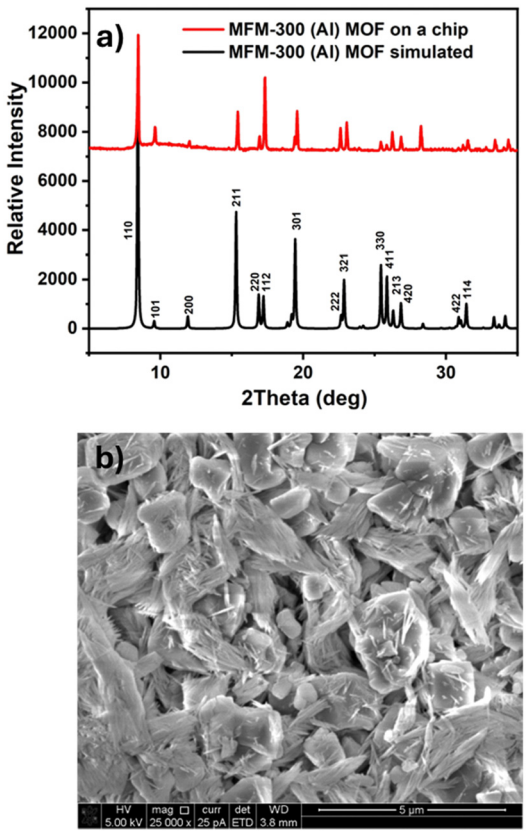

Fig. 1 (a) Calculated X-ray diffraction (XRD) patterns of the NOTT-300 (Al) MOF (black) and thin film deposited on the IDE substrate (red) and (b) top view SEM image of the thin film.

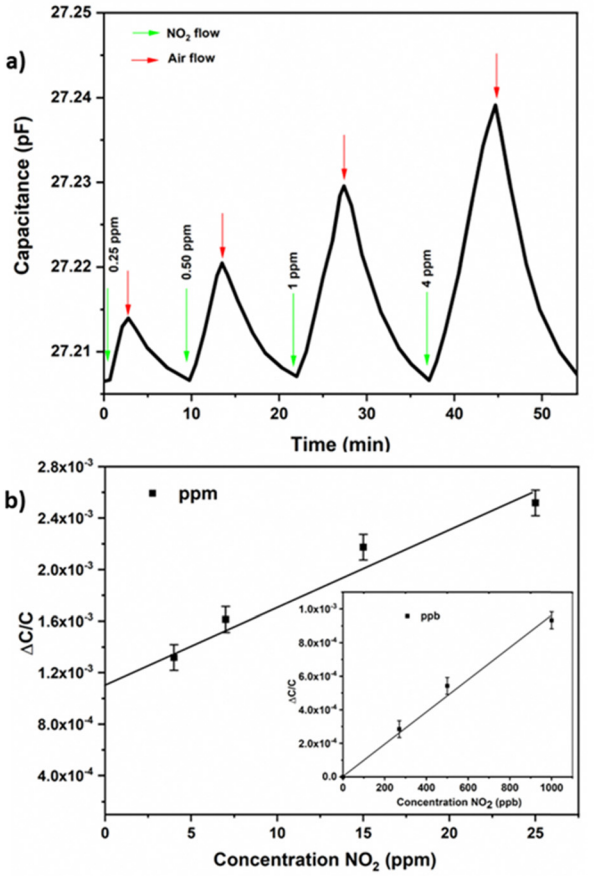

Fig. 2 (a) Dynamic response–recovery curve of the NOTT-300 (Al) MOF sensor to different concentrations of NO_2. (b) The detection of NO_2 in different concentration ranges: 250 ppb–4 ppm and (inset) 250–1000 ppb linear response for the corresponding range.

The stability of the NOTT-300 (Al) MOF sensor for NO_2 detection at room temperature was demonstrated using reproducibility tests, through which the performance of the sensors for detecting 4, 1, 0.5, and 0.25 ppm of NO_2 within a testing period of two weeks (Fig. 3) was observed. The aforementioned tests demonstrate the stability of the NOTT-300 (Al) MOF sensor and its superior NO_2 detection. The temperature (T) dependence of NO_2 sensitivity for the NOTT-300 (Al) MOF sensor was also studied in the temperature range of 35–55 °C (Fig. 4). The sensitivity response as expected has logically decreased with the temperature increase because, in the NOTT-300 (Al) MOF, as in most materials, equilibrium sorption decreases with increasing temperature and the best sensitivity was obtained at 35 °C. Further, upon increasing the temperature from 35 °C to 55 °C, we observed a drop of almost 24%, which can be attributed to the reduced interaction capability of the active sites, which leads to the increase of molecular diffusion and weakened their interaction with the framework, leading to a decrease in the sorption amount.

The evaluation of the sensor's selectivity for NO_2 was conducted under conditions that mimicked real atmospheric conditions. These experiments were performed in the presence of varying relative humidity (RH%) values and diverse concentrations of CO_2 (Fig. 5).

Firstly, the effect of relative humidity (RH) on the performance of the MOF sensor was investigated. The humidity in the chamber was adjusted to the desired level (26–60% RH) and capacitance response was considered as the new baseline (Fig. S3, ESI†). Then at each RH level, the capacitance change was recorded in the presence of NO_2 at 250 ppb until 8 ppm. Distinctive signals for NO_2 concentrations (Fig. 5(b)) at a RH of 26% were seen for concentrations starting from 0.5 ppm, which is slightly reduced compared to what had been observed in "dry" conditions (Fig. 2a), which confirms the strong affinity of the NOTT-300 (Al) MOF sensor to NO_2 and its practical applicability in the presence of water molecules. The sensor performance in higher humidity conditions like 47% and 60% was still acceptable, and concentrations down to 5 ppm were still detectable. In addition, a relatively small increase of the sensor response with an increase of RH may be attributed to the dissolution of NO_2 molecules into the physiosorbed water on the MOF layer.[34]

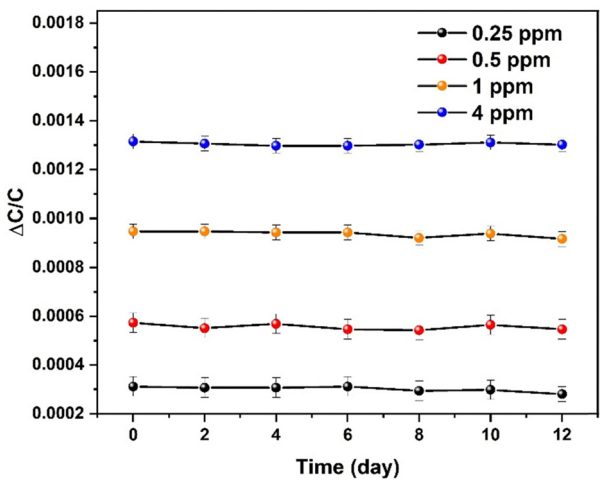

Fig. 3 The stability performance of the Al-NOTT-300 MOF sensor over a time period of 12 days.

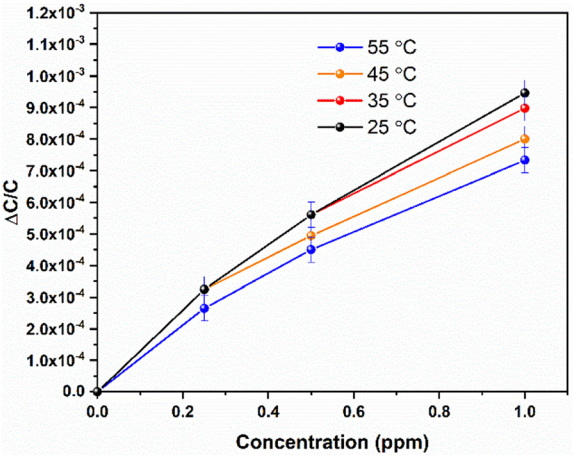

Fig. 4 NOTT (Al) 300 MOF sensor response under various NO_2 concentrations as a function of the working temperature.

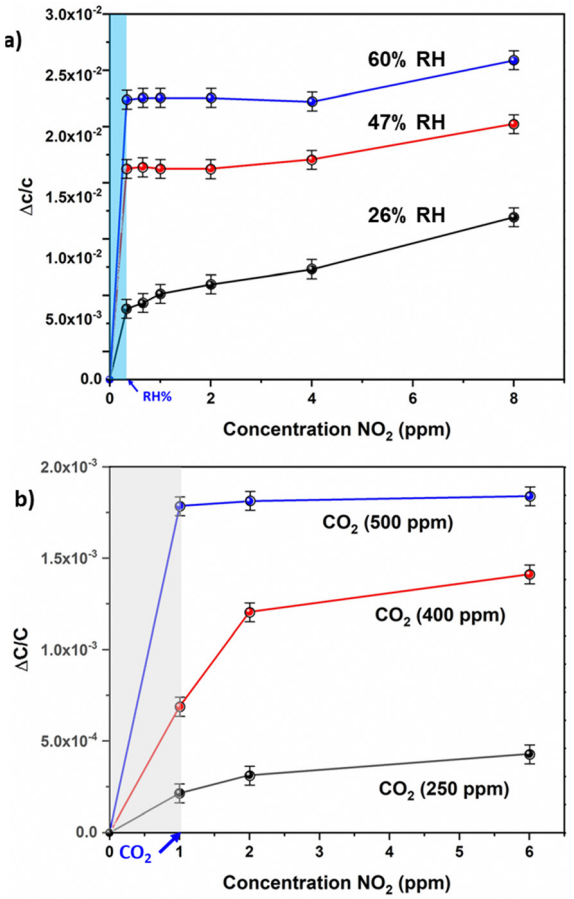

Fig. 5 Effects of various exposure conditions: (a) variable relative humidity ranging from 26 to 60% RH and (b) variable CO_2 concentrations ranging from 250 to 500 ppm on the performance of the Al-NOTT-300 sensor.

Secondly, the effect of carbon dioxide (CO_2) on the performance of the MOF sensor was investigated.[32] The CO_2 concentration in the chamber was adjusted to the desired level (250–500 ppm), and capacitance response was considered as the new baseline (Fig. S4, ESI†). Then at each CO_2 concentration, the capacitance change was recorded in the presence of NO_2 from 1 to 6 ppm. Distinctive signals for NO_2 concentrations (Fig. 5(a)) at 250 ppm CO_2 were seen for concentrations starting from 3 ppm, which confirms the strong affinity of the Al-NOTT-300 MOF sensor to NO_2 and its practical applicability in the presence of CO_2 molecules.

The sensor performance at higher CO_2 concentrations like 400 ppm was still acceptable; however; at 500 ppm NO_2, concentrations down to 5 ppm were not detectable. Finally, the NOTT-300 MOF (Al) based sensor showed an excellent sensitivity for NO_2 even in the presence of 26% humidity, and a 500 ppm CO_2 mixture (Fig. S4, ESI†), still low concentrations down to 5 ppm of NO_2 are still achievable. These results testify the great selectivity of NO_2 in the presence of other gases/vapors with different physical and chemical properties.

The newly reported NO_2 MOF sensor demonstrates exceptional affinity for NO_2, coupled with cost effective and easily achievable capacitive measurements, resulting in superior NO_2 sensing capabilities. Consequently, these findings present promising prospects for the development of enhanced sensors utilizing capacitance or alternative transduction mechanisms.

Conclusion

In conclusion, in this study we have demonstrated the excellent performance of the NOTT-300 (Al) MOF as a sensing layer thin film on a capacitive IDE sensor for NO_2 detection at room temperature. Principally, the NOTT-300 (Al) MOF sensor offers distinctive NO_2 detection at concentrations down to 250 ppb with a limit of detection of 4.0 ppb. The stability of the NOTT-300 (Al) MOF sensor was confirmed using different methods. The signal intensity associated with the NOTT-300 (Al) MOF sensor for NO_2 detection was compared to the corresponding signal in the presence of relevant gases/vapours, such as water and CO_2, and it reveals the distinctive and remarkable sensing selectivity of the NOTT-300 (Al) MOF sensor towards NO_2. This reveals that the unique sensing feature of the NOTT-300 (Al) MOF sensor paves the way for the application of MOFs as useful sensors for various prominent applications.

Data availability

Data supporting this study are included within the article and/or the ESI.†

Conflicts of interest

There are no conflicts of interest to declare.

Acknowledgements

The authors acknowledge the King Abdullah University of Science and Technology for funding this project.

References

1 D. J. Wales, J. Grand, V. P. Ting, R. D. Burke, K. J. Edler, C. R. Bowen, S. Mintova and A. D. Burrows, *Chem. Soc. Rev.*, 2015, **44**, 4290–4321.
2 J. R. Stetter, W. R. Penrose and S. Yao, *J. Electrochem. Soc.*, 2003, **150**, 11–16.
3 L. Zhang, P. De Schryver, B. De Gusseme, W. De Muynck, N. Boon and W. Verstraete, *Water Res.*, 2008, **42**, 1–12.
4 K.-H. Kim, Y. Choi, E. Jeon and Y. Sunwoo, *Atmos. Environ.*, 2005, **39**, 1103–1112.
5 K.-H. Kim, E.-C. Jeon, Y.-J. Choi and Y.-S. Koo, *Atmos. Environ.*, 2006, **40**, 4478–4490.
6 J. Lelieveld, T. Butler, J. Crowley, T. Dillon, H. Fischer, L. Ganzeveld, H. Harder, M. Lawrence, M. Martinez and D. Taraborrelli, *Nature*, 2008, **452**, 737–740.
7 P. M. Edwards, S. S. Brown, J. M. Roberts, R. Ahmadov, R. M. Banta, W. P. Dubé, R. A. Field, J. H. Flynn, J. B. Gilman and M. Graus, *Nature*, 2014, **514**, 351–354.
8 Z. Chen, J.-N. Wang, G.-X. Ma and Y.-S. Zhang, *Lancet Neurol.*, 2013, **382**, 1959–1960.
9 S. J. Tans, A. R. M. Verschueren and C. Dekker, *Nature*, 1998, **393**, 49.
10 J. Hahm and C. M. Lieber, *Nano Lett.*, 2004, **4**, 51–54.
11 C. Li, D. Zhang, X. Liu, S. Han, T. Tang, J. Han and C. Zhou, *App. Phys. Lett.*, 2003, **82**, 1613–1615.
12 J. Li, Y. Lu, Q. Ye, M. Cinke, J. Han and M. Meyyappan, *Nano Lett.*, 2003, **3**, 929–933.
13 J. Kong, N. R. Franklin, C. Zhou, M. G. Chapline, S. Peng, K. Cho and H. Dai, *Science*, 2000, **287**, 622–625.
14 S. F. Chen, A. Aldalbahi and P. X. Feng, *Sensors*, 2015, **15**, 27035–27046.
15 A. Mane, S. Kulkarni, S. Navale, A. Ghanwat, N. Shinde, J. Kim and V. Patil, *Ceram. Int.*, 2014, **40**, 16495–16502.
16 W. Bracke, P. Merken, R. Puers and C. Van Hoof, *IEEE Trans. Circuits Syst.*, 2007, **54**, 130–140.
17 H.-C. Zhou, J. R. Long and O. M. Yaghi, *Chem. Rev.*, 2012, **112**, 673–674.
18 L. E. Kreno, K. Leong, O. K. Farha, M. Allendorf, R. P. Van Duyne and J. T. Hupp, *Chem. Rev.*, 2011, **112**, 1105–1125.
19 V. Chernikova, O. Shekhah, Y. Belmabkhout, M. Karunakaran and M. Eddaoudi, *Angew. Chem.*, 2023, **135**, e2022188.
20 H. Sohrabi, S. Ghasemzadeh, Z. Ghoreishi, M. R. Majidi, Y. Yoon, N. Dizge and A. Khataee, *Mat. Chem. Phys.*, 2023, **299**, 127512.
21 N. Alsadun, S. Surya, K. Patle, V. S. Palaparthy, O. Shekhah, K. N. Salama and M. Eddaoudi, *ACS Appl. Mater. Interfaces*, 2023, **15**, 6202–6208.
22 D. Masih, V. Chernikova, O. Shekhah, M. Eddaoudi and O. F. Mohammed, *ACS Appl. Mater. Interfaces*, 2018, **10**,

11399–11405; C. Sapsanis, H. Omran, V. Chernikova, O. Shekhah, Y. Belmabkhout, U. Buttner, M. Eddaoudi and K. N. Salama, *Sensors*, 2015, **15**, 18153–18166.
23 O. Yassine, O. Shekhah, A. H. Assen, Y. Belmabkhout, K. N. Salama and M. Eddaoudi, *Angew. Chem., Int. Ed.*, 2016, **55**, 15879–15883.
24 A. H. Assen, O. Yassine, O. Shekhah, M. Eddaoudi and K. N. Salama, *ACS Sens.*, 2017, **2**, 1294–1301.
25 V. Chernikova, O. Yassine, O. Shekhah, M. Eddaoudi and K. N. Salama, *J. Mater. Chem. A*, 2018, **6**, 5550–5554.
26 X. Han, H. G. Godfrey, L. Briggs, A. J. Davies, Y. Cheng, L. L. Daemen, A. M. Sheveleva, F. Tuna, E. J. McInnes and J. Sun, *Nat. Mater.*, 2018, **17**, 691–696.
27 S. Yang, L. Liu, J. Sun, K. M. Thomas, A. J. Davies, M. W. George, A. J. Blake, A. H. Hill, A. N. Fitch and C. C. Tang, *J. Am. Chem. Soc.*, 2013, **135**, 4954–4957.
28 V. Tsouti, M. Filippidou, C. Boutopoulos, P. Broutas, I. Zergioti and S. Chatzandroulis, *Procedia Eng.*, 2011, **25**, 835–838.
29 O. Shekhah, C. Busse, A. Bashir, F. Turcu, X. Yin, P. Cyganik, A. Birkner, W. Schuhmann and C. Wöll, *Phys. Chem. Chem. Phys.*, 2006, **8**, 3375–3378.
30 J. Li, Y. Lu, Q. Ye, M. Cinke, J. Han and M. Meyyappan, *Nano Lett.*, 2003, **3**, 929–933.
31 M. Savage, Y. Cheng, T. L. Easun, J. E. Eyley, S. P. Argent, M. R. Warren, W. Lewis, C. Murray, C. C. Tang and M. D. Frogley, *Adv. Mater.*, 2016, **28**, 8705–8711.
32 P. Xu, T. Xu, H. Yu and X. Li, *Anal. Chem.*, 2017, **89**, 7031–7037.
33 I. Sasaki, H. Tsuchiya, M. Nishioka, M. Sadakata and T. Okubo, *Sens. Actuators, B*, 2002, **86**, 26–33.
34 M. R. Tchalala, Y. Belmabkhout, K. Adil, K. N. Chappanda, A. Cadiau, P. M. Bhatt, K. N. Salama and M. Eddaoudi, *ACS Appl. Mater. Interfaces*, 2018, **11**, 1706–1712.